Improved Map-Slice-to-Volume Motion Correction with B0 Inhomogeneity Correction: Validation of Activation Detection Algorithms Using ROC Curve Analyses

Desmond T.B. Yeo[1,2], Roshni R. Bhagalia[1,2], and Boklye Kim[1]

[1] Department of Radiology, University of Michigan Medical School, MI 48109, USA
{tbyeo, rbhagali, boklyek}@umich.edu
[2] Department of Electrical Engineering and Computer Science, University of Michigan, MI 48109, USA

Abstract. Head motion is a significant source of error in fMRI activation detection and a common approach is to apply 3D volumetric rigid body motion correction techniques. However, in 2D multislice fMRI, each slice may have a distinct set of motion parameters due to inter-slice motion. Here, we apply an automated mutual information based slice-to-volume rigid body registration technique on time series data synthesized from a T_2 MRI brain dataset with simulated motion, functional activation, noise and geometric distortion. The map-slice-to-volume (MSV) technique was previously applied to patient data without ground truths for motion and activation regions. In this study, the activation images and area under the receiver operating characteristic curves for various time series datasets indicate that the MSV registration improves the activation detection capability when compared to results obtained from Statistical Parametric Mapping (SPM). The effect of temporal median filtering of motion parameters on activation detection performance was also investigated.

1 Introduction

Head motion is a significant source of error in fMRI activation detection, particularly in regions with strong intensity edges. In fMRI, activation detection techniques typically rely on test statistics that quantify voxel intensity differences between activated and rest states. Since the intensity change due to the BOLD effect is only about 1% to 4%, any motion induced intensity change can severely degrade the activation detection performance. This limitation may yield misleading functional mapping and preclude patients with severe motor control pathologies from participating in fMRI experiments. Several retrospective motion correction techniques have been applied to multislice fMRI data [1,2] and most of them involve 2D to 2D, 3D volumetric or slice-stack registration where 3D inter-slice motion is ignored. In the map-slice-to-volume (MSV) approach [3], each single-shot EPI slice in the time series is spatially repositioned into an anatomical reference space. In previous work [3], it was shown that the accuracy of registration parameters attained by MSV on noiseless simulated T_2 International Consortium of Brain Mapping (ICBM) data without geometric distortion is in the range of -0.10±0.07º and -0.07±0.03mm (mean±standard error of mean). In addition, test results of human subjects performing the unilateral motor task

R. Larsen, M. Nielsen, and J. Sporring (Eds.): MICCAI 2006, LNCS 4191, pp. 276 – 283, 2006.

suggest improved localization of functional activation compared to the slice-stack registration approach. However, the activation detection performance could not be quantified since there was no known ground truth in the clinical data used.

In this work, we seek to evaluate the accuracy of MSV in activation detection of noiseless and noisy time series images with simulated motion and activation regions. The results are compared with Statistical Parametric Mapping (SPM) activation results from the same datasets. We also investigate the effects of temporal filtering of motion parameter estimates on activation detection performance in the presence and absence of field inhomogeneity induced geometric distortion. For comprehensive motion correction and activation detection, several synthetic T_2 time series datasets with simulated motion, functional activation regions, noise and geometric distortion were simulated with known ground truths for the activated regions and the six degree-of-freedom (DOF) rigid body motion parameters for each slice. Statistical activation maps of the datasets with and without MSV motion correction and temporal filtering are computed and used to generate receiver operating characteristic (ROC) curves. The area under each ROC curve quantifies the activation detection accuracy.

2 Methods

2.1 Map Slice-to-Volume Motion Correction

The MSV motion correction technique models the 3D motion of multislice EPI data by allowing each slice to have its own six DOF rigid body motion [3]. Each slice $\boldsymbol{f}^l$ is registered with a 3D anatomical reference volume $\boldsymbol{g}_{ref}$ using the rigid body transform T_{α^l} where $\boldsymbol{\alpha}^l$ denotes a vector of six MSV rigid body motion parameters t_x, t_y, t_z, θ_x, θ_y, θ_z for slice l. To estimate $\boldsymbol{\alpha}^l$, the negated mutual information (MI) cost function

$$\Psi_1(\boldsymbol{\alpha}^l) = -\mathrm{MI}(\boldsymbol{g}_{ref}, \boldsymbol{f}^l(T_{\boldsymbol{\alpha}^l}(\boldsymbol{r}))) \ , \tag{1}$$

which measures the dissimilarity between $\boldsymbol{f}^l$ and $\boldsymbol{g}_{ref}$, is minimized using the Nelder-Mead downhill simplex optimization algorithm. Registration using an MI-based cost function is especially appropriate for multi-modality datasets, i.e. T_2^*-weighted EPI slices registered with a T_1 anatomical reference volume. After registration, each set of optimized motion parameters is used to transform and interpolate (trilinear) its respective slice $\boldsymbol{f}^l$ into a volume with the same spatial coordinates as the reference volume. The motion of each slice is thus computed independent of other slices. Intra-slice motion is ignored since it is typically negligible for single shot acquisitions.

Given that head motion is typically correlated in time and that MSV may generate outlier estimates due to local minima in the cost function, it may be helpful to perform temporal filtering on the raw MSV motion parameter estimates prior to reconstructing the slices into the reference volume. As an example, Fig. 1 shows raw and median filtered MSV estimates of a rotation parameter θ_x from a T_2 time series dataset using a filter window of nine samples. The ground truth is 0º for all slices.

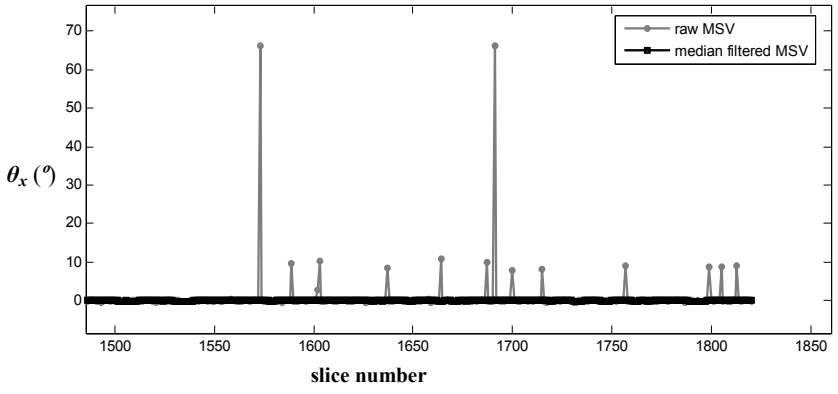

Fig. 1. Recovered rotation parameter θ_x from raw MSV estimates (RMSE: 4.00°) and median filtered MSV estimates (RMSE: 0.04°) from a dataset with no motion in θ_x

2.2 Activation Detection with Random Permutation Test (RPT)

After reconstructing all the slices into volumes, MSV yields time series volumes that may have empty voxels. This results in variable temporal sample sizes for different voxels for statistical analysis. The non-parametric statistical method of voxel-wise random permutation, using the averaged difference between activation and rest images as the test statistic, was used for significance testing of differences in voxel intensities in the simulated datasets [3]. This statistical technique is simple, robust and independent of sample size variability [6]. Random draws of 2000 permutations of activated and rest periods were used to form a permutation distribution for each voxel from which activated regions are identified by testing the null hypothesis of no activation at a fixed threshold of P = 0.001. To obtain ROC curves, we vary the threshold P values from 10^{-4} to 1.0 to obtain a set of activation maps and, together with the ground truth activation map, compute the true positive and false alarm rates. The area under each ROC curve measures how accurately the activation regions have been detected.

2.3 Iterative Field-Corrected Image Reconstruction

To perform EPI geometric distortion correction, we use an iterative field-corrected reconstruction method that, unlike many non-iterative image reconstruction methods, does not assume a smooth field-map [4]. The continuous object $\boldsymbol{f}^l$ and field-map $\Delta\omega$ are parameterized into a sum of weighted rect functions $\varphi(\boldsymbol{r}\text{-}\boldsymbol{r}_n)$ where $\boldsymbol{r}$ is the vector of spatial coordinates. Ignoring spin relaxation and assuming uniform receiver coil sensitivity, the matrix-vector form of the parameterized MR signal equation for slice l in an EPI time series can be written as follows:

$$\boldsymbol{u}^l = \boldsymbol{A}^l \boldsymbol{f}^l + \boldsymbol{\varepsilon}^l \tag{2}$$

with elements of the system-object matrix $\boldsymbol{A}^l$ expressed as

$$a^l_{m,n} = \Phi(\boldsymbol{k}(t_m)) e^{-j\Delta\omega^l_n t_m} e^{-j2\pi(\boldsymbol{k}(t_m)\cdot\boldsymbol{r}_n)} \tag{3}$$

where $\boldsymbol{\varepsilon}^l$ denotes white Gaussian noise, $\Phi(\boldsymbol{k}(t_m))$ denotes the Fourier transform of $\varphi(\boldsymbol{r}\text{-}\boldsymbol{r}_n)$, $\Delta\omega_n{}^l$ is field-inhomogeneity value at $\boldsymbol{r}_n$. To estimate the unknown slice $\boldsymbol{f}^l$ from the k-space data, the iterative conjugate gradient algorithm is used to minimize

$$\Psi_2(\boldsymbol{f}^l) = \left\|\boldsymbol{u}^l - \boldsymbol{A}^l\boldsymbol{f}^l\right\|^2 + \beta\left\|\boldsymbol{C}\boldsymbol{f}^l\right\|^2 \tag{4}$$

where $\boldsymbol{C}$ is the first-order difference matrix and β is a parameter that controls the tradeoff between obtaining a data-consistent estimate and a smoothed estimate.

In order to achieve accurate field-corrected reconstruction of the time series images with head motion, every slice of observed data $\boldsymbol{u}^l$ should be paired with a dynamic field map slice $\Delta\omega^l$ that tracks the motion-induced field-inhomogeneity changes during the fMRI experiment. However, since only a static field-map, $\Delta\omega_{static}$, is typically available, we use re-sampled slices of $\Delta\omega_{static}$ in place of $\Delta\omega^l$ to perform the geometric distortion correction. This does not take into account field map changes in the presence of head motion during the fMRI experiment.

2.4 Motion, Activation and Geometric Distortion Data Simulation

To simulate the datasets, two perfectly registered T_1- and T_2-weighted image datasets (matrix size: 256×256×124, voxel size: 0.8mm×0.8mm×1.5mm) derived from ICBM data were used. The T_1 volume is used as the anatomical reference for MSV registration and the T_2 volume forms the "baseline" volume from which the time series datasets are simulated. To simulate functional activation, an "activated" T_2 volume was created by increasing the T_2 ICBM dataset intensity by 5% in selected ground truth ellipsoidal regions as shown in Fig. 4(c). In addition, a simulated brain static field map was created by adding three 3D Gaussian blobs located at the inferior frontal and inferior temporal lobes to a 3D third order polynomial. The field inhomogeneity map was scaled to have a maximum value of 5ppm at 1.5T.

Six baseline-activation cycles, each formed by concatenating ten baseline volumes and ten activated T_2 volumes, were assembled to form a 120-volume time series. Temporally continuous motion in three rotation parameters, θ_x, θ_y and θ_z, was applied to the T_2 time series as well as the simulated field map volumes and sequential 5.6mm thick slices were then re-sampled to form 14-slice volumes (matrix size: 256×256×14). Each re-sampled slice has its own set of motion parameters. The simulated motion has maximum values of 5.0°, 8.6° and 8.1° for θ_x, θ_y and θ_z respectively. Four such time series datasets with motion were simulated with slice acquisition interleaving. Different combinations of simulated noise, field-inhomogeneity induced geometric distortion and distortion correction were then applied to these datasets.

To forward distort the T_2 images, simulated Cartesian blipped EPI k-space data of the distorted images was generated with the field map time series with motion using Eq. 2. The distorted images were then reconstructed from this k-space data using a system-object matrix with a field map set to zero [5]. The simulated readout time was 43.8ms and the pixel bandwidth in the phase encode direction was 22.8Hz. The final four simulated time series datasets are denoted by **D1** for T_2 without noise, **D2** for T_2 with additive 5% Rayleigh noise (σ=2.83), **D3** for T_2 without noise but with geometric distortion with a simulated field map (5ppm) with motion, and **D4** for dataset **D3** after iterative field-corrected image reconstruction with a static field map. Fig. 2

summarizes how the datasets were generated. It is noted that dataset **D3** was simulated with the assumption that the field map moves with a rigid body transformation function with the head and does not model local field map changes with out-of-plane motion.

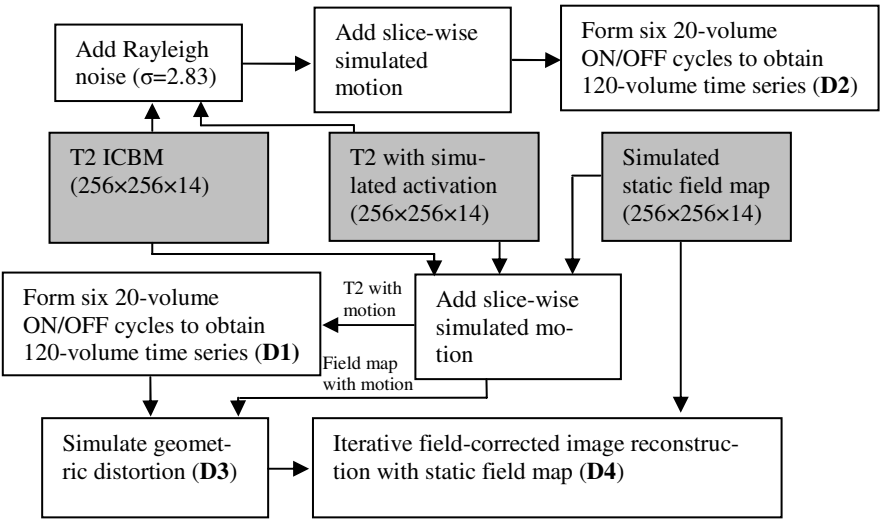

Fig. 2. Flowchart of simulated time series datasets **D1**, **D2**, **D3** and **D4**

3 Experiments and Results

In the first set of experiments, the objective is to quantify the improvement in activation detection with MSV corrected data compared to SPM generated results. Thus, MSV motion correction was applied to datasets **D1** and **D2** and a random permutation test with 2000 random permutations of activated and rest states was used to generate activation maps for various P values from which ROC curves were computed. ROC curves were also computed from t-statistic maps generated by SPM on the same datasets. In the second set of experiments, the objective is to investigate if temporal median filtering improves activation detection for noiseless datasets **D1**, **D3** and **D4**. Thus, each dataset is corrected with raw MSV and median filtered MSV motion parameters to yield two separate time series datasets. Activation detection is then performed on these two datasets using the random permutation test.

3.1 Activation Detection Performance with MSV-RPT and SPM

Table 1 summarizes the area under the ROC curve (AUC) values for both sets of experiments. For datasets **D1** and **D2**, it is observed that the AUC values of raw MSV corrected data (first column) are higher than those from SPM corrected data (third

column). The increase is 0.041 and 0.070 for noiseless and noisy T_2 data respectively. This improvement is reflected in the ROC plots in Fig. 3(a).

Table 1. Area under ROC curves for time series data processed with various methods

Dataset	Area Under ROC Curves (AUC)		
	Raw MSV	MSV with median filtering	SPM
(**D1**) Noiseless T_2	0.967	0.967	0.926
(**D2**) Noisy T_2	0.958	0.955	0.888
(**D3**) Distorted T_2	0.909	0.915	-
(**D4**) Distortion corrected T_2	0.930	0.930	-

Fig. 4 shows several slices of the ground truth activation together with detected activation regions for MSV corrected data and SPM processed data. It is observed that MSV corrected data yielded a significantly larger number of true positives.

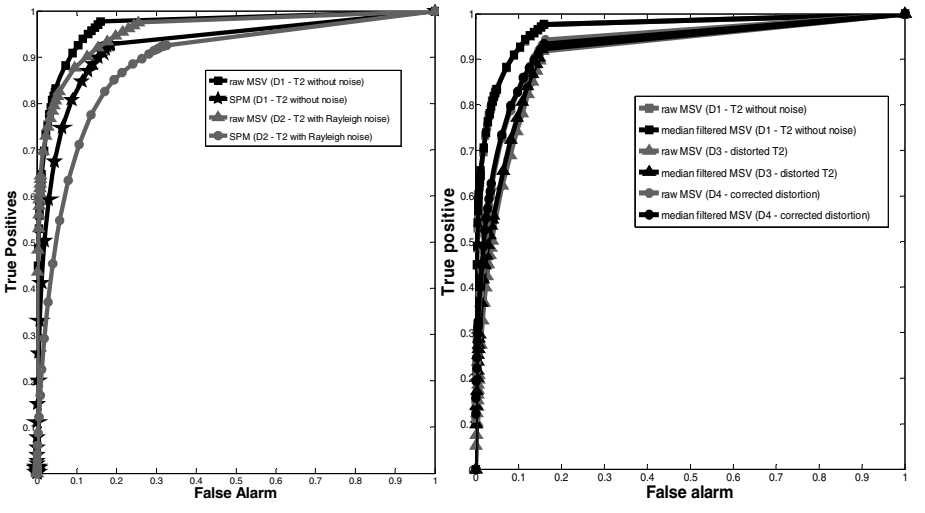

(a) **(b)**

Fig. 3. ROC curves for time series datasets (**a) D1** and **D2** to compare MSV and SPM, (**b**) **D1, D3** and **D4** to observe effects of temporal median filtering on ROC curves

3.2 Temporal Filtering of MSV Motion Parameters

Table 2 shows that the RMSE values for the various datasets decrease significantly with median filtering. However, Table 1 shows that the AUC values of datasets corrected with median filtered MSV estimates are not much different from those of datasets corrected with raw MSV estimates, with the exception of the geometrically distorted dataset **D3**. Fig. 3(b) shows the respective three pairs of ROC curves.

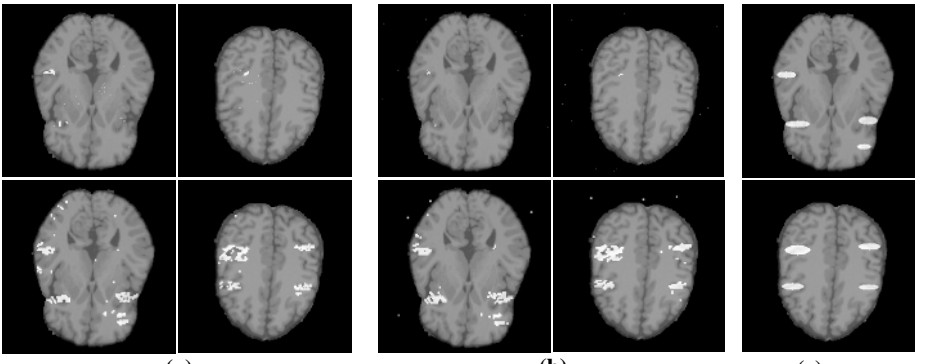

Fig. 4. Detected activation regions for (**a**) noiseless T_2 with motion (**D1**), (**b**) T_2 with motion and Rayleigh noise (**D2**). Rows show activation maps of respective T_2 time series datasets processed with SPM (top), MSV (bottom) with random permutation test. (**c**) Ground truth simulated activation regions of the two sample slices.

Table 2. RMSE of motion parameter estimates with and without median filtering

Dataset	RMSE (mm and º)											
	MSV without median filtering						MSV with median filtering					
	t_x	t_y	t_z	θ_x	θ_y	θ_z	t_x	t_y	t_z	θ_x	θ_y	θ_z
D1	1.2	1.0	0.7	2.2	2.4	2.0	1.2	1.0	0.7	0.2	0.2	0.1
D2	1.2	1.0	0.7	0.3	0.2	0.1	1.2	1.0	0.7	0.2	0.2	0.1
D3	2.0	7.6	1.9	2.9	1.6	1.0	1.4	7.8	1.0	1.0	0.5	0.4
D4	1.2	3.3	0.6	0.3	0.4	0.2	1.1	3.2	0.5	0.2	0.2	0.2

4 Discussion and Conclusions

In this paper we evaluated the activation detection performance when a voxel-wise random permutation test is applied to MSV corrected datasets and compared it to the performance of SPM. We also investigated the effects of temporal filtering of MSV estimates for various types of datasets.

Table 1 shows that the AUC values for MSV corrected data are higher than those from SPM datasets, especially in the presence of image noise. It is highly likely that the improvement came about largely because the built-in motion correction algorithm in SPM does not model 3D inter-slice motion. This quantified observation provides additional evidence that activation detection accuracy can be improved by applying retrospective MSV motion correction to fMRI time series images prior to statistical testing. It was also observed that temporal median filtering does not change the AUC values significantly except in the distorted dataset **D3** (Table 1). This could be due to the larger number of outlier estimates as reflected in the higher variance and, in part, higher RMSE values of the motion parameter estimates in the presence of geometric distortion in dataset **D3** (Table 2). In the other datasets without geometric distortion, outlier motion estimates occur much less frequently and thus, median filtering may

not have much effect on activation detection since the intensity errors due to reconstructed slices with outlier motion parameter estimates tend to be averaged out when computing the mean difference test statistic in the random permutation test. The results suggest that while temporal filtering may yield estimates that are closer to the physical head motion, it may improve activation detection only in slices with significant field inhomogeneity related distortions, i.e., temporal cortex language area. Future work will investigate specific conditions in which temporal filtering of MSV estimates will benefit activation detection. A comparison of SPM AUC values for **D3** and **D4** will also be done to evaluate MSV for geometrically distorted datasets.

Acknowledgements

This work was supported in part by the National Institute of Health grants 1P01 CA87634 and 8R01 EB00309. We are grateful to Dr. Jeffrey A. Fessler for his iterative field-corrected image reconstruction software and to the anonymous reviewers for their constructive comments.

References

1. Friston, K.J., Ashburner, J., Frith, C.D., Poine, J.B., Heather, J.D., Frackowiak, R.S.J.: Spatial registration and normalization of images. Hum. Brain Map. **2** (1995) 165-189
2. Jiang, A.P., Kennedy, D.N., Baker, J.R.,Weisskoff, R., Tootell, R.B.H., Woods, R.P., Benson, R.R., Kwong, K.K., Brady, T.J., Rosen, B.R., Beliveau, J.W.: Motion detection and correction in functional MR imaging. Hum. Brain Map. **3** (1995) 224-35
3. Kim, B., Boes, J.L., Bland, P.H., Chenevert, T.L., Meyer, C.R.: Motion correction in fMRI via registration of individual slices into an anatomical volume. Magn. Reson. Med. **41** (1999) 964-972
4. Sutton, B.P., Noll, D.C., Fessler, J.A.: Fast, iterative image reconstruction for MRI in the presence of field inhomogeneities. IEEE Trans. Med. Imag. **22** (2003) 178-188
5. Yeo, D.T.B., Fessler, J.A., Kim, B.: Concurrent geometric distortion correction in mapping slice-to-volume (MSV) motion correction of fMRI time series. In: Barrillot, C., Haynor, D., Hellier, P. (eds.): Proc. Of MICCAI'04. Lecture Notes in Computer Science, Vol. 3217. Springer-Verlag, Berlin Heidelberg New York (2004) 752-760
6. Good, P.: Permutation tests. Springer-Verlag, Berlin Heidelberg New York (1994)